Journal of Pharmaceutical and Biomedical Analysis 55 (2011) 1067–1074

Contents lists available at ScienceDirect

Journal of Pharmaceutical and Biomedical Analysis

journal homepage: www.elsevier.com/locate/jpba

Metabonomics study of the protective effects of green tea polyphenols on aging rats induced by D-galactose

Chunwang Fu[a], Tiejie Wang[b], Yang Wang[c], Xiaohui Chen[c], Jian Jiao[c], Feng Ma[a], Min Zhong[b], Kaishun Bi[c,*]

[a] School of Traditional Chinese Materia Medica, Shenyang Pharmaceutical University, Shenyang 110016, PR China
[b] Shenzhen Institute for Drug Control, Shenzhen 518057, PR China
[c] School of Pharmacy, Shenyang Pharmaceutical University, Wenhua Road 103, Shenyang 110016, PR China

ARTICLE INFO

Article history:
Received 21 January 2011
Received in revised form 5 March 2011
Accepted 5 March 2011
Available online 11 March 2011

Keywords:
Metabonomics
Green tea polyphenols
Anti-aging
D-Galactose
UPLC/MS

ABSTRACT

This article was designed to study metabonomic characters of aging induced by D-galactose (D-gal) and the protective effects of green tea polyphenols (GTP). Plasma samples from control, D-gal and GTP treated rats were analysed by ultra-performance liquid chromatography coupled with mass spectrometry (UPLC/MS) in positive mode. Coupled with biochemistry and histopathology results, the significant difference in metabolic profiling between D-gal treated group and the GTP treated group by using the principal components analysis (PCA) indicated that changes in global plasma metabolites were occurred. Some significantly changed metabolites like lysophosphatidylcholines, tryptophan, dihydrosphingosine and phytosphingosine have been found and identified. These changes in plasma metabolites are related to the perturbations of lecithin metabolism, amino acid metabolism and phospholipids metabolism, which may be helpful to further understand the action mechanisms of GTP.

1. Introduction

Aging, an aspect of almost all living organism, is a multifactorial process of enormous complexity and is characterized by impairment of various cellular modulation and functions, affecting various systems such as nervous system and immune system [1]. It is an inevitable biological process that eventually causes many chronic age-associated diseases, including cancer, cardiovascular diseases and neurodegenerative diseases. Anti-aging has already become a major public issue as the elderly population increases in the world.

Accumulated evidence has shown that the generation of free radical or reactive oxygen species (ROS) can lead to cell and tissue damage, resulting in aging and ultimately cell death [2]. Indeed, with the aging increasing, the antioxidative defense system include enzymes such as superoxide dismutase (SOD), catalase (CAT), glutathione reductase (GR), glutathione peroxidase (GPx) and non-enzymatic antioxidants such as ascorbate, a-tocopherol and glutathione decline during the aging process [3], accordingly, oxidative stress induced by an overproduction of ROS leads to a disruption of cellular macromolecules functions, such as DNA, proteins and lipids of cell membranes [4]. Oxidative stress plays an important role during the pathogenesis of aging and age-associated diseases [5]. Antioxidant supplementation has been proved to be an ameliorator of oxidative stress [6]. Dietary antioxidants, in particular, green tea polyphenols (GTP) has been found beneficial in protecting against the generation of ROS. GTP is a group of polyphenolic compounds extracted from green tea (*Camellia sinensis*), a widely consumed beverage in many countries around the world, especially in China and Japan. It has been reported that the main active components of GTP are flavanols, commonly known as tea catechins including (−)-epigallocatechin-3-gallate (EGCG), (−)-epicatechin-3-gallate (ECG), (−)-epigallocatechin (EGC), (−)-epicatechin (EC), (+)-gallocatechin (GC) and (+)-catechin (C). Numerous studies have revealed that GTP possesses the potent radical scavenging, iron-chelating and also indirectly through modulation of transcription factors or enzymes [7,8] and has wide health promoting properties, such as anti-aging, anti-artherosclerosis and the cancer chemopreventive effects [9–11]. Until now, many works on the pharmacological mechanism of GTP mainly focus on gene expression, cell morphology, as well as biochemical and pathological changes studies. While, few are known about the change of the whole metabolites in an organism treated with GTP. Neither has it been experimentally investigated how GTP affects the metabolism of whole body.

Metabonomics is an important platform of systems biology, defined as the quantitative measurement of the dynamic multiparametric metabolic response of living systems to patho-

* Corresponding author. Tel.: +86 24 23986296; fax: +86 24 23986259.
E-mail address: bikaishun@yahoo.com (K. Bi).

0731-7085/$ – see front matter © 2011 Elsevier B.V. All rights reserved.
doi:10.1016/j.jpba.2011.03.011

physiological stimuli or genetic modifications [12]. The ability to measure global alteration in metabolism in biological fluids and tissues is well coincident with the integrity and systemic feature of traditional Chinese medicine, which precedes conventional biochemical and pathological changes, has contributed to the emergence of metabonomics as a promising scientific platform for understanding the biochemical basis of diseases, drug toxicity, the diagnosis and treatment of diseases [13,14]. However, there is no report on the molecular biomarkers for anti-aging effects of GTP with a metabonomic approach.

Recent metabonomic technologies based on mass spectrometry (MS) and nuclear magnetic resonance (NMR) are all powerful analytical tools to measure low molecular weight metabolites in biological samples. Compared with NMR, MS is inherently considerable more sensitive than NMR spectrometry. When MS is coupled with ultra performance liquid chromatography (UPLC), high sensitivity, high resolution, wide dynamic range, coverage of a wide chemical diversity, robustness and feasibility to elucidate the molecular weight and structure of unknown compounds can be achieved for the low abundance metabolites. UPLC/MS has been used for observing the subtle metabolic changes under some diseases or treatment of diseases and provided informative data for elucidating biochemical basis of diseases and addressing the therapeutic effect of medicines [15,16].

It was reported that chronic D-galactose (D-gal) exposure could induce memory loss, neurodegeneration, oxidative damage and impair neurogenesis in the dentate gyrus, a process similar to the natural aging in mouse [17,18]. Rodent chronically injected with D-gal has been used as an animal aging model for anti-aging research and health food testing [19].

Based on the reasons above, in this article, aging model rats were established by injecting the male Wistar rats intraperitoneally with D-gal once a day. Corresponding plasma samples were collected from control rats, D-gal treated rats and GTP treated rats for the metabonomic analysis by using UPLC/MS system. Principal component analysis (PCA) was performed for investigating the metabolic changes among the plasma of rats, here, we study the effects of GTP in the aging rats and explore potential molecular biomarks for the anti-aging effects of GTP using metabonomic method.

2. Experimental

2.1. Chemicals and reagents

Acetonitrile and formic acid were HPLC grade (NJ, Fisher Corp., USA), water was purified by redistillation and was filtered through 0.22 μm membrane filter before use. The standard of tryptophan was purchased form Sigma–Aldrich (Sigma Corp., Mo, USA). Green tea polyphenols was purchased from Zhejiang Orient Tea Development Company (Hangzhou, China). The purity of green tea polyphenols was 98%, the content of EGCG was 75.2%, EGC was 2.62%, EC was 1.51%, ECG was 9.7%, GC was 5.95%, C was 3.19%, gallic acid was 1.02% and caffeine was 0.81% in GTP (by HPLC-UV). The total antioxide capacity (T-AOC), total superoxide dismutase (T-SOD), glutathione reductase (GR), glutathione peroxidase (GPx), catalase (CAT) and malondialdehyde (MDA) commercial kits were purchased from Nanjing Jiancheng Institute of Biotechnology (Nanjing, China). D-galactose was purchased from Sigma–Aldrich (Sigma Corp., Mo, USA). The D-galactose was dissolved in physiological saline (0.9% saline and distilled water) at concentration of 20 mg/mL.

2.2. Animals and treatment

35 male Wistar rats of 6 week-old weighing 200–220 g from Shanghai Slack Laboratory Animal Co. Ltd., were used in the study. Animal care was in accordance with the Guidelines for Animal Experimentation of Shenyang Pharmaceutical University (Shenyang, China) and the protocol was approved by the Animal Ethics Committee of the institution. The animals were fed with a certified standard diet and tap water *ad libitum*, and were allowed to acclimate for a period of 1 week before the experiment. During the study, all animals were kept in animal room with temperature: 18–21 °C, humidity: 45–65%, and 12 h dark to light cycle. To reduce contamination, the rats were placed in clean cages each day. After 1 week of acclimatization, all rats were randomly divided into 5 groups (n = 7/group): control group (CG); D-gal group (DG); high dosage group of GTP (HG); middle dosage group of GTP (MG) and low dosage group of GTP (LG). The rats of DG, HG, MG and LG received injection of D-gal intraperitoneally at a dose of 100 mg/(kg/day) for 8 weeks, from the fifth week, all rats of LG, MG and HG received daily GTP at a dose of 200, 400 and 800 mg/(kg/day) in distilled water by oral gavage for another 4 weeks, respectively; and the rats of control group (CG) received injection of physiological saline intraperitoneally and oral gavage with the approximately same volume distilled water as the other groups.

2.3. Sample collection and preparation

After 8 weeks treatment, blood samples of CG, DG, HG, MG and LG rats were collected from the suborbital vein into heparinized tubes and immediately centrifuged at 3000 rpm for 10 min. The plasma was transferred into clean tubes and stored at −20 °C until analysis.

Prior to analysis, the plasma samples were thawed at room temperature, then centrifuged at 15,000 rpm for 10 min. Acetonitrile (400 μL) was added to plasma (200 μL) and vortex-mixed vigorously for 3 min, then centrifuged at 15,000 rpm for 10 min at 4 °C. The supernatant was pipetted out and evaporated to dryness at 30° C under a gentle stream of nitrogen. The dried residue was then reconstituted in 200 μL of acetonitrile-water (15:85, v/v) and vortex-mixed for UPLC/MS analysis.

2.4. Biochemical assay

Rats were deeply anesthetized and then sacrificed by decapitation. Brains were prompted removed and dissected on ice to obtain the hippocampus, frozen in liquid nitrogen and stored at −80 °C until further processing. The activities of T-AOC, T-SOD, GR, GPx, CAT and the level of MDA were determined by using commercially available kits. All procedures completely complied with the manufacture′s instructions.

2.5. Histopathology

For histological evaluation, rats were deeply anesthetized with 10% chloral hydrate, and the brain was infused with physiological saline. After perfusion fixation with paraformaldehyde, the brain was removed and stored in fixative for 24 h, then embedded in paraffin wax and sectioned at 5 μm. Sections of hippocampal CA1 area were stained with hematoxylin and eosin.

2.6. Chromatography

Liquid chromatography was performed on ACQUITY™ UPLC system (Waters Corp., Milford, MA, USA) equipped with cooling autosampler and column oven. Chromatographic separation was

Table 1
Gradient elution program of UPLC/MS.

Time (min)	Flow rate (mL/min)	A% (0.1% FA-ACN)	B% (0.1% FA-water)
Initial	0.2	15	85
1	0.2	28	72
6	0.2	70	30
7	0.2	90	10
8	0.2	100	0
11	0.2	100	0
12	0.2	15	85

performed on a 5 cm × 2.1 mm ACQUITY 1.7 μm C_{18} column maintained at 35 °C, 5 μL sample solution was injected to the column for each run. The UPLC mobile phase consisted of 0.1% formic acid in acetonitrile (solution A) and 0.1% formic acid in water (solution B). The gradient elution program was shown in Table 1.

2.7. Mass spectrometry

The mass spectrometric data were collected on a Micromass Quattro micro™ API mass spectrometer (Milford, MA, Waters Corp., USA) with an electrospray ionization (ESI) interface and triple quadruple mass analyser. Mass spectra were obtained on a fullscan operation in positive ion mode. The capillary voltage was set at 3.0 kV, and the cone voltage was optimized at 30 V. The source temperature of 120 °C, a desolvation gas temperature of 350 °C, and nitrogen was used as desolvation and cone gas with the flow rate of 600 and 50 L/h, respectively. Data profiling of positive ions from *m*/*z* 100 to 900 was recorded at a speed of 1 s/scan with 0.1 s as the inter-scan delay during analysis. In the MS/MS experiments, argon was employed as the collision gas and collision energy was set from 10 eV to 30 eV. The data were collected in centroid mode, and the mass was corrected with NaCsI before the study.

For accurate mass analysis, metabolites were performed on Waters Micromass QTof-micro™ (Waters Corp., Manchester, UK) equipped with an electrospray source operating in positive ion mode. The desolvation gas was set to 500 L/h at a temperature of 250 °C. The cone gas was set to 25 L/h and the source temperature was set to 90 °C. The capillary and cone voltages were set to 2.6 kV and 30 V, respectively. The data acquisition rate was set to 0.4 s, with a 0.1 s inter-scan delay. All analyses were acquired using the lock spray to ensure accuracy and reproducibility. Leucine enkephalin was used as the lock mass (*m*/*z* 556.2771) at a concentration of 0.2 ng/μL. Data were collected in centroid mode. The lock spray frequency was set at 5 s and data were averaged over 10 scans for correction.

2.8. Data analysis

The mass data acquired were imported to Markerlynx (Waters, UK) within Masslynx software (version 4.0) for peak detection and alignment. The retention time and *m*/*z* data for each peak were determined by the software. The parameters of Markerlynx method were set as follows: mass tolerance 0.1 Da; noise elimination level 5; full scan mode was employed in the mass range of 100–900 amu; the initial and final retention time was set as 0 min and 12 min for data collection. All data were normalized to the summed total ion intensity per chromatogram, and the resultant data matrices were introduced to SIMCA-P 10.0 software package (Umetrics, Umea, Sweden) for principal component analysis (PCA). PCA was conducted on mean-centered, pareto-scaled data from the plasma samples. Mean centering subtracts the average from the data sets columnwise, thereafter resulting in a shift of the data towards the mean. Pareto scaling gives each variable a variance equal to the square root of its standard deviation. One of the main reasons for using the pareto-scaling method is that such procedure is a satisfactory comprise between UV-scaling (scaling to unit variance), which gives equal weight to the baseline noise and individual signals in the entire chromatogram, and no scaling, which could fail to pick out small changes in metabolites with lower concentrations. While pareto scaling technique enhances the contribution of lower concentration metabolites without amplifying noise and artifacts commonly present in the metabonomic data sets, which is positive for the models' predictive ability [20].

2.9. Identification of the endogenous metabolites

All collected plasma samples were analyzed and low molecular weight metabolites were represented as the chromatographic peaks in the total ion current (TIC) chromatograms. Mass spectra were interpreted with available biochemical databases, such as KEGG (http://www.genome.jp/kegg/), METLIN (http://metlin.scripps.edu/), and HMDB (http://www.hmdb.ca/). The collision induced dissociation (CID) experiment was implemented to get fragmentation patterns of these potential plasma biomarkers. Furthermore, identification of metabolites was performed using the commercial available standards by comparing their MS spectra and retention time. Meanwhile, some biomarkers were also identified by the retention time and the accurate mass number of Waters ESI-QTOF-MS under the same liquid chromatography condition.

3. Result and discussion

3.1. Biochemistry and histopathology results

To evaluate the oxidative stress and the level of lipid peroxidation in hippocampus, the activities of major antioxidant enzymes and MDA level had been tested. As Fig. 1 reports, the activities of T-AOC, T-SOD, GPx, CAT and GR were markedly decreased after exposed to D-gal for 8 weeks compared with CG, and all these increases were obvious improved by GTP in different groups, and the effect in HG was most obvious. The content of MDA indirectly reflects the level of lipid peroxidation production, which was significantly increased in DG, but these changes were significantly intervened by GTP only in MG and HG, while HG was more stronger.

Hematoxylin–eosin staining was used to survey the histopathological changes after chronic intraperitoneal administration of D-gal and the GTP treatment. In CG, neuronal cell were laid in closer with large nuclei and clear nucleoli (Fig. 2A). Marked morphological changes were visualized in DG (Fig. 2B): neuronal cell loose, cell karyopyknosis and dark staining of neurons. In contrast, the pathological abnormalities were gradually ameliorated in the GTP treated groups, and the effect of HG was most noticeable, which almost showed normal histology with large nuclei and clear nucleoli (Fig. 2E).

Taken together, all these results showed that the aging animal model of D-gal treated rats was successfully reproduced and the GTP was demonstrated to intervene its effects positively, and the action of HG was mostly strong, so metabolic profiling in following experiments only paid close attention to the blood samples of high dose group rats.

3.2. Method development and method validation

A protein precipitation step was used prior to the metabolic profiling analysis by UPLC/MS to extract low-molecular-weight compounds nonconvalently bound to proteins and remove the large amount of proteins present in the plasma that would otherwise interfere with the final UPLC/MS analysis. The volume ratio of sample to precipitation reagent (acetonitrile) was investigated.

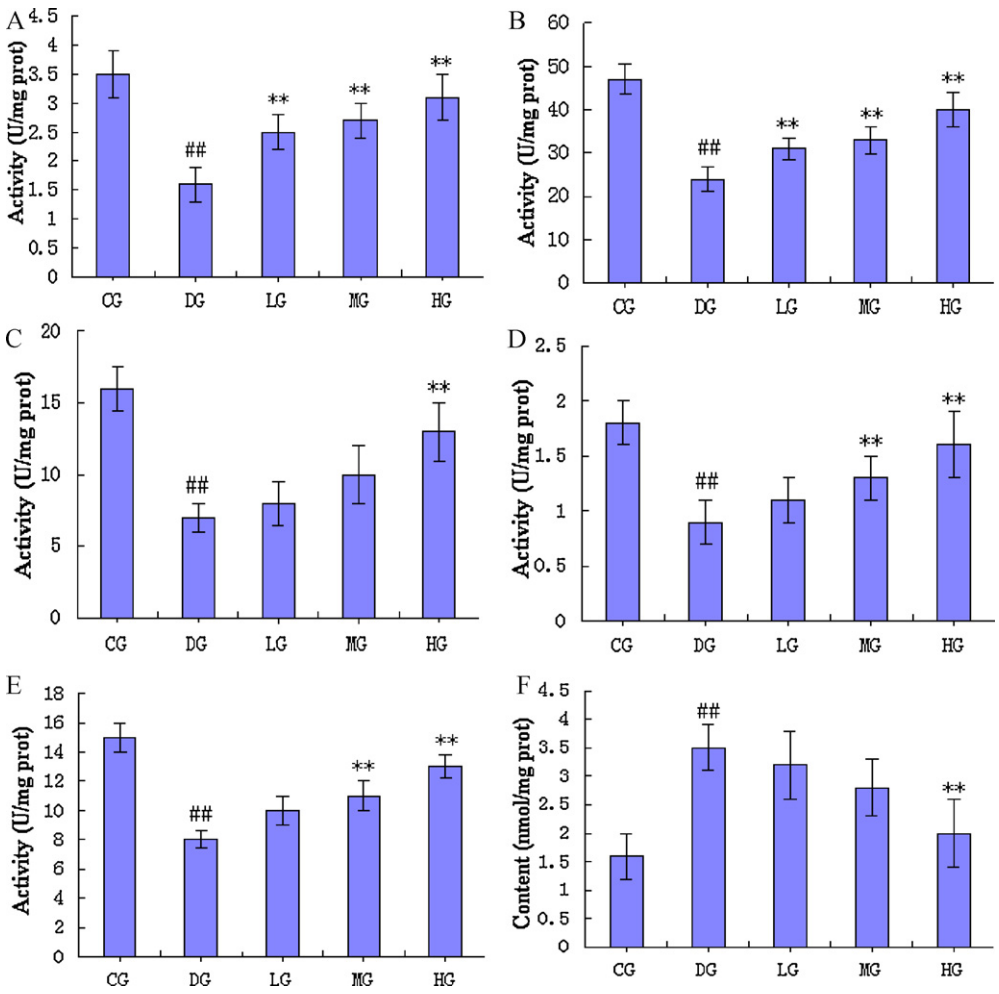

Fig. 1. Effects of D-galactose and green tea polyphenols on activities of T-AOC (A), T-SOD (B), GPx (C), CAT (D), GR (E) and content of MDA in rats hippocampus. The data were expressed as mean ± S.D. ##Significant difference compared with CG groups ($p < 0.01$) and **significant difference compared with DG groups ($p < 0.01$).

Compared with the ratio of 1:1, more peaks were observed in base peak intensity (BPI) chromatograms in the ratio of 1:2 and 1:3, and no significant difference between 1:2 and 1:3. The ratio of 1:2 was select for easier evaporation. Acetonitrile was chosen as the organic phase, furthermore, the effects of acid modifier (formic acid) with different concentrations (1, 0.1 and 0.01%) were characterized, the optimal peak resolution and shape were obtained by 0.1% formic acid. Full scan of plasma metabolites were set in the positive ion mode. The contents in the GTP were also analyzed by UPLC/MS. No detectable peaks assignable to the GTP and its metabolites were

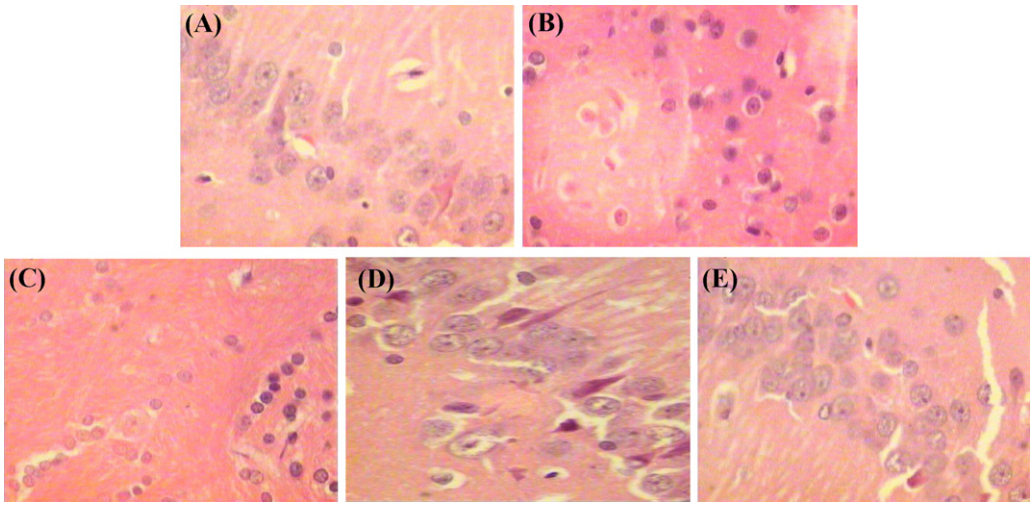

Fig. 2. Effects of D-galactose and green tea polyphenols on histopathological changes in rats hippocampus CA1 area. (A) CG hippocampus CA1; (B) DG hippocampus CA1; (C) LG hippocampus CA1; (D) MG hippocampus CA1 and (E) HG hippocampus CA1. Magnification 400×.

observed on the UPLC/MS chromatograms of the plasma from control rats.

For method validation study, 100 μL each of all the plasma samples studied were pooled to generate a pooled quality control (QC) sample containing all the analytes that would be encountered during the analysis. Extracted ion chromatographic peaks of ten ions were selected according to their chemical polarities and *m*/*z* values. The paired retention time_*m*/*z* of these ions were 2.1_218.1, 2.8_274.2, 3.4_415.1, 3.8_302.3, 4.5_520.3, 5.2_496.3, 5.5_330.3, 7.2_524.4, 8.3_282.3 and 9.9_338.3 in positive ion mode with retention times covering the whole analytical time for method validation. Precision of injection was evaluated by the continuous detection of six replicates of the same QC sample. Precision of injection (R.S.D.%) of these selected peaks areas, retention times and *m*/*z* were estimated to be 2.2–6.1%, 0.053–0.61% and 0–0.012%, respectively. Then six parallel samples were prepared for the repeatability of sample preparation study. Method repeatability (R.S.D.%) of peaks areas, retention times and *m*/*z* of ten selected ions were 2.4–7.6%, 0–0.77% and 0–0.011%, respectively. The system stability was carried out by injecting a QC sample every 5 samples during the whole sample analysis. System stability (R.S.D.%) of peaks areas, retention times and *m*/*z* of these selected ions were 2.5–8.1%, 0.071–0.91% and 0–0.012%, respectively. The good precision, repeatability and stability indicated that the method could be utilized to the analysis of plasma samples.

3.3. Analysis of metabolic profiling

Fig. 3 presents the representative positive ion BPI chromatograms of typical plasma sample from control rat, D-gal treated rat and GTP treated rat. Although some differences could be visually noted among the three sets of detail illustrated in the TIC chromatograms, more subtle changes could be visualized by using pattern recognition approach. Principle component analysis (PCA) is a non-supervised multivariate data analysis method and it gives the comprehensive view of the clustering trend for the multidimensional data. In order to gain an overview of the rat plasma metabolic profiling, here, PCA was used in the subsequent UPLC/MS data analysis. To determinate whether the GTP was possible to influence metabolic pattern of D-gal treated rats and to find the metabolites with a significant concentration change (i.e. potential biomarkers), we conducted a model using PCA. The validity of the PCA model was assessed by the correlation coefficient R^2 and the cross-validation correlation coefficient Q^2. R^2 is defined as the proportion of variance in the data explained by the models and indicates goodness of fit. Q^2 is defined as the proportion of variance in the data predictable by the model and indicates predictability. Fig. 4A shows that in the scores plot, the D-gal treated model group and control group can be clearly separated. The results indicated that the plasma metabolic pattern was significantly changed in the D-gal treated aging model group. It also can be seen from the PCA score plot, the GTP treated group located between the model group and the control group, and much closer to the control group. The PCA score plot revealed good fitness and high predictability of the PCA model with high statistical values of R^2 (0.73) and Q^2 (0.65), respectively.

Based on the result of showed by the PCA score plot, coupled with biochemistry and histopathology results, some conclusions could be made as follows: the aging model induced by D-gal was established, and the aging was being prevented and alleviated, exhibiting a tendency recovering to healthy control group after taking green tea polyphenols.

3.4. Biomarker elucidation

The loading plot from the PCA based on UPLC/MS data (5479 variables) was shown in Fig. 4B. The distance of an ion from the origin represents the contribution to the clustering of different groups on the PCA. A number of ions which were found predominantly in the loading plot, with retention time and *m*/*z* pairs of 0.5_205.3, 2.9_318.3, 3.8_302.3, 4.4_542.3, 4.5_520.3, 4.5_544.3, 5.2_496.3, 7.2_524.4 and 8.4_568.6 were chosen as biomarkers. Here, we take *m*/*z* 318.3 as an example to illustrate the identification process. In positive ion spectrum (Fig. 5A), besides the base peak ion at *m*/*z* 318.3, the ions at *m*/*z* 340.4 was found. Thus, we infer that the quasi-molecular ion is *m*/*z* 318.3 ($[M+H]^+$) and the ion at *m*/*z* 340.4 is the adduction ($[M+Na]^+$). The ion at *m*/*z* 316.3 in negative ion mode (Fig. 5B) further validated the metabolite has a molecular mass of 317.3 Da. With different collision energies, the corresponding MS/MS information was obtained. In positive product ion scan spectrum (Fig. 5C), the ions like 318, 300, 282 and 264 were found. Each of them has the difference of water, which indicated that there must be three hydroxyl groups in structure. To define its structure, some databases like KEGG (http://www.genome.jp/kegg/) and HMDB (http://www.hmdb.ca/) were searched with the molecular weight 317.3 Da, then some compounds without three hydroxyl groups were removed from the candidate list. Furthermore, under the same liquid chromatogra-

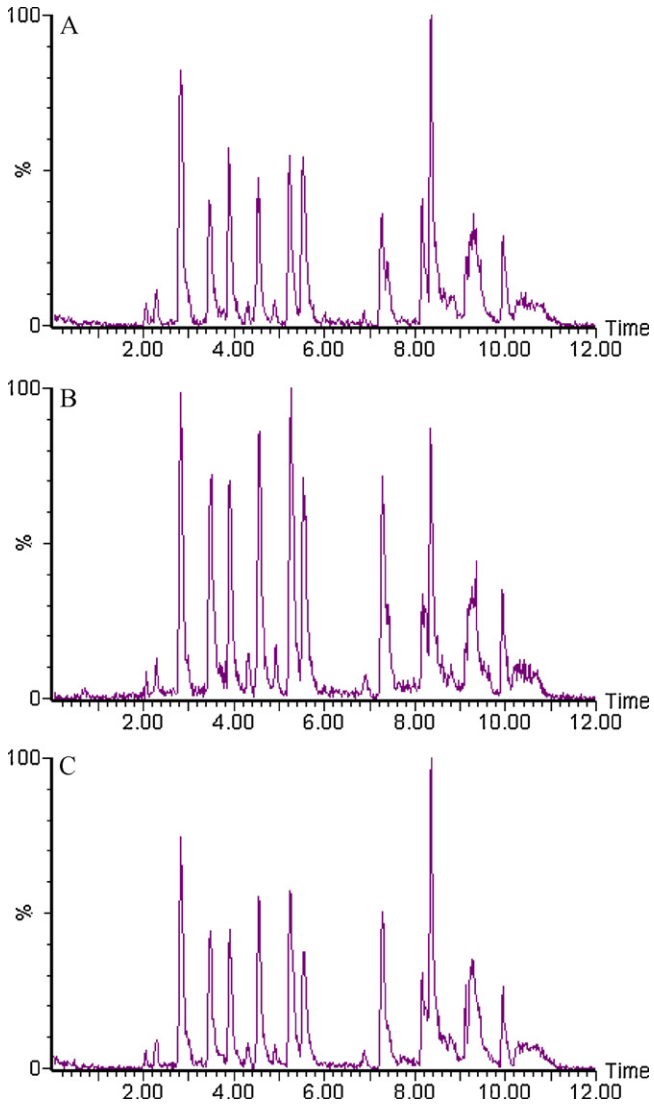

Fig. 3. Positive ion base peak intensity (BPI) chromatograms of representative plasma sample from (A) control rat, (B) D-galactose treated rat and (C) green tea polyphenols treated rat.

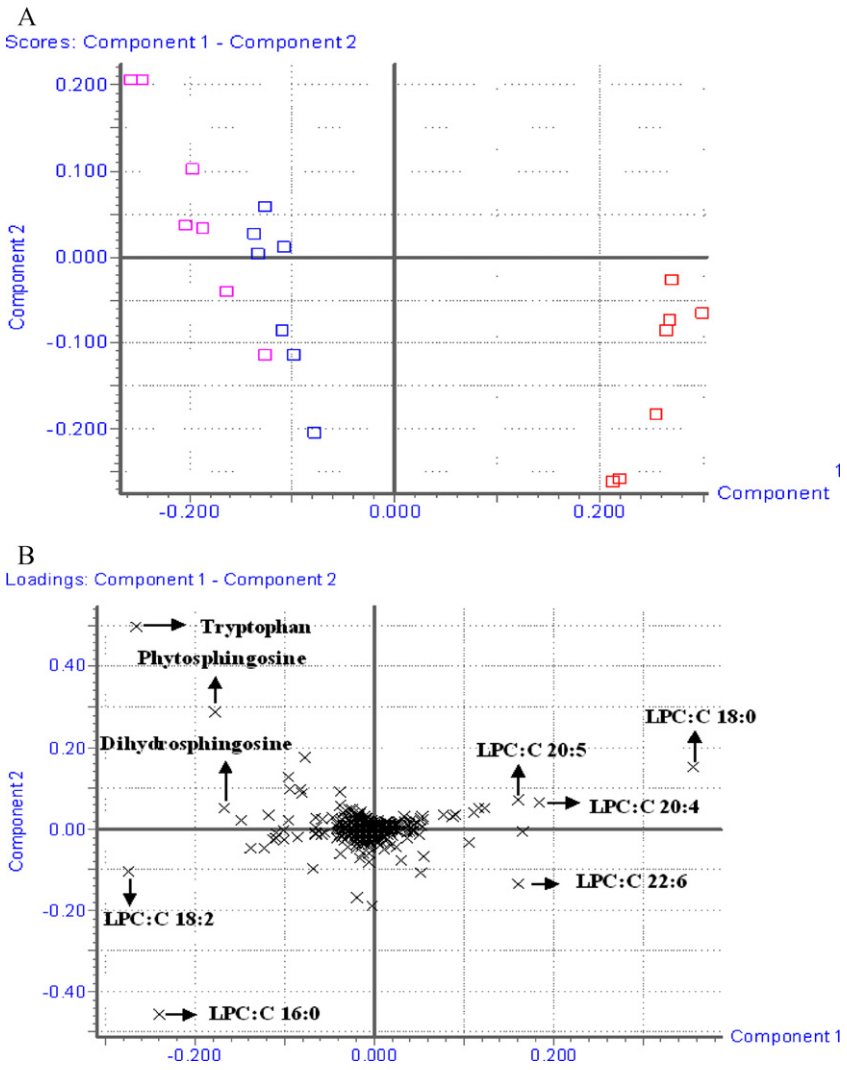

Fig. 4. (A) PCA score plot and (B) loading plot based on the plasma metabolic profiling of the control rat (□), green tea polyphenols treated rat (□) and D-galactose treated rat (□). (For interpretation of the references to colour in this figure legend, the reader is referred to the web version of this article.)

phy condition, the sample was injected to water's ESI-QTOF-MS, at the same retention time, accurate molecular weight *m/z* 318.3004 (theoretical *m/z* 318.3003, error 0.31 ppm, in HMDB) was found and it was the only peak in the extracted ion chromatogram (*m/z* 318). Finally, it was tentatively identified as phytosphingosine. By using the same method described above, nine potential biomarkers were identified. Table 2 lists the potential biomarkers identified for classifying aging rats and rats treated with GTP.

Table 2
Identification results of potential biomarkers detected by UPLC/MS.

Retention time	*m/z*	Scan mode	Quasi-molecular ion	Metabolites	Change trend of GTP treated rats vs. aging rats
5.2	496.3	+	$[M+H]^+$	LPC16:0	↓
	540.3	–	$[M+HCOO]^-$		
4.5	520.3	+	$[M+H]^+$	LPC18:2	↓
	564.3	–	$[M+HCOO]^-$		
7.2	524.4	+	$[M+H]^+$	LPC18:0	↓
	568.4	–	$[M+HCOO]^-$		
4.4	542.3	+	$[M+H]^+$	LPC20:5	↓
	586.3	–	$[M+HCOO]^-$		
4.5	544.3	+	$[M+H]^+$	LPC20:4	↓
	588.3	–	$[M+HCOO]^-$		
8.4	568.6	+	$[M+H]^+$	LPC22:6	↓
	612.7	–	$[M+HCOO]^-$		
0.5	205.3	+	$[M+H]^+$	Tryptophan	↑
	203.3	–	$[M-H]^-$		
3.8	302.3	+	$[M+H]^+$	Dihydrosphingosine	↓
	300.4	–	$[M-H]^-$		
2.9	318.3	+	$[M+H]^+$	Phytosphingosine	↓
	316.3	–	$[M-H]^-$		

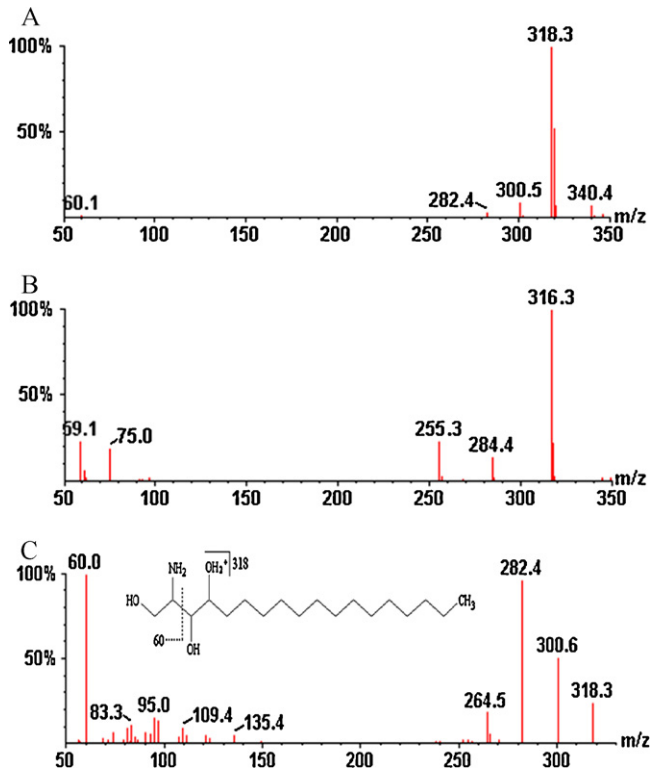

Fig. 5. Mass spectra of biomarker at (A) *m/z* 318.3 in positive ion mode, (B) *m/z* 316.3 in negative ion mode and (C) product ion scan spectrum of the biomarker in positive ion mode.

3.5. Biochemical interpretation

Table 2 gives the change trends of the metabolites identified by UPLC/MS, in the plasma of GTP treated rats compared with untreated ones. The results effectively indicated that these metabolites may be the biomarkers of anti-aging effects of GTP, which were related to the action mechanism of GTP.

This study indicated that lysophosphatidylcholine was obviously increased in aging rats and decreased in the GTP treated rats, and the reason is not clear completely; however, one of the most important theories of aging is related to free radicals [2]. Much attention has been focused on the involvement of oxidative stress in the aging process, and age-related diseases, such as Parkinson's disease and Alzheimer's disease. When oxidative stress occurred, the generation of free radical can activate the phospholipase A_2, which could hydrolyse phosphatidylcholine to produce lysophosphatidylcholine, nevertheless, the potent free radical scavenging ability of the GTP can inhabit phospholipase A_2 activities. This fact may explain the increasing trend of lysophosphatidylcholine in aging rats and the decreasing trend of GTP treated rats. Furthermore, lysophosphatidylcholine is the potent detergent-like cytotoxic compound, which can damage plasmalemma and vesicular membranes and may eventually cause cell death if occurring in sufficient quantity [21].

Tryptophan is essential amino acid which cannot be synthesized by the body. It is either incorporated into proteins or broken down for energy and metabolic intermediates. Tryptophan is the precursor of serotonin, which is an important neurotransmitter. Change of the amino acid in aging rats may indicate an alteration of the balance between nutrition intake and consumption. The increase of energy and protein expenditure could be the main reasons for the decrease of tryptophan. Based on our study, compared with the aging group, tryptophan increased remarkably in GTP treated rats, which may showed that aging progress is involved in amino acid metabolism.

Dihydrosphingosine and phytosphingosine are classified into sphingolipids, and play important roles in the sphingolipids biosynthesis and metabolism. The first step involved in sphingolipid biosynthesis is initiated by the condensation of serine and palmitoyl-CoA results in the formation of dihydrosphingosine. Subsequently, dihydrosphingosine is linked with fatty acyl group to generate dihydroceramide. Introduction of the 4–5 double bond by a desaturase then results in the formation of ceramide, which has been implicated in cellular aging processes [22]. In our study, an obvious increase of dihydrosphingosine and phytosphingosine in aging rats and decrease in the GTP treated group was observed. As membrane components, sphingolipids might be among the first cell components to encounter extracellular stressors; indeed, much evidence implicates sphingolipids in cell adaptation to stress. In the specific stress conditions, including oxidative stress and radiation stress, chemical or thermal stress, and starvation, which initiate changes in sphingolipid metabolism [23]. Sphingolipids have emerged as key mediators of stress responses by canonical (protein kinase activation or inhibition and G-protein-coupled receptor signaling) and non-canonical (components of lipid platforms and initiation of membrane pore formation) paradigms [24]. Extracellular stressors induce sphingolipid synthesis and accumulation, thereby "remodeling" sphingolipid profiles and their topological distribution within cells [25]. Intensive investigation in the past decade has firmly established the role of sphingolipids in controlling signal pathways for cell survival [26] and aging [27]. However, in many cases, mechanistic information remains scarce, thus, further study of sphingolipid-mediated etiology represents a crucial challenge, and the specific mechanism responsible for the GTP-induced sphingolipids reduction needs further research.

4. Conclusion

In this study, UPLC/MS was employed in the metabonomic study of biochemical changes in the plasma of aging rats induced by D-gal after the treatment of GTP. With the PCA, a clear separation of model group and control group was achieved. The GTP treated group located between the model group and the control group, and much closer to the control group. Furthermore, several potential biomarkers like lysophosphatidylcholines, tryptophan, dihydrosphingosine and phytosphingosine for aging rats induced by D-galactose and protection by GTP were found and identified. Combined with biochemistry and histopathology results, the changes in plasma metabolites indicated the perturbations of lecithin metabolism, amino acid metabolism and phospholipids metabolism are related to aging induced by D-gal and the interventions of GTP on all the three metabolic pathways. This work demonstrates that metabonomics is a potentially powerful tool for identifying and characterizing biochemical responses of rat to chemicals (e.g., D-galactose). Meanwhile, this strategy offers a comprehensive method for performing intervened assessments of traditional Chinese medicines. If it can be combined with genomics, transcriptomics and proteomics study, metabonomics will give a better and further understanding of the efficacy and mechanism research of traditional Chinese medicines in the future.

Acknowledgement

The author gratefully thanks Dr. Wentao Liu, Dr. Chao Ma and Junhong Ling (Shenyang Pharmaceutical University, PR China) for the valuable suggestions and support during the experiment.

References

[1] K. Kawakami, J. Kadota, K. Iida, R. Shirai, K. Abe, S. Kohno, Reduced immune function and malnutrition in the elderly, Tohoku J. Exp. Med. 187 (1999) 157–171.
[2] D. Harman, Aging: a theory based on free radical and radiation chemistry, J. Gerontol. 11 (1956) 298–300.
[3] G. Murali, C. Panneerselvam, Age-associated oxidative macromolecular damages in rat brain regions: role of glutathione monoester, J. Gerontol. A: Biol. Sci. Med. Sci. 62 (2007) 824–830.
[4] D. Haripriya, P. Sangeetha, A. Kanchana, M. Balu, C. Panneerselvam, Modulation of age-associated oxidative DNA damage in rat brain cerebral cortex, striatum and hippocampus by L-carnitine, Exp. Gerontol. 40 (2005) 129–135.
[5] F.B. Johnson, D.A. Sinclair, L. Guarente, Molecular biology of aging, Cell 96 (1999) 291–302.
[6] C.A. Rice-Evans, A.T. Diplock, Current status of antioxidant therapy, Free Radic. Biol. Med. 15 (1993) 77–96.
[7] C. Cabrera, R. Artacho, R. Giménez, Beneficial effects of green tea—a review, J. Am. Coll. Nutr. 25 (2006) 79–99.
[8] J.V. Higdon, B. Frei, Tea catechins and polyphenols: health effects, metabolism, and antioxidant functions, Crit. Rev. Food Sci. Nutr. 43 (2003) 89–143.
[9] Q. Meng, C.N. Velalar, R. Ruan., Effects of epigallocatechin-3-gallate on mitochondrial integrity and antioxidative enzyme activity in the aging process of human fibroblast, Free Radic. Biol. Med. 44 (2008) 1032–1041.
[10] T. Yokozawa, T. Nakagawa, K. Kitani, Antioxidative activity of green tea polyphenol in cholesterol-fed rats, J. Agric. Food. Chem. 50 (2002) 3549–3552.
[11] J.D. Lambert, C.S. Yang, Cancer chemopreventive activity and bioavailability of tea and tea polyphenols, Mutat. Res. 523 (2003) 201–208.
[12] J.K. Nicholson, J.C. Lindon, E. Holmes, Metabonomics: understanding the metabolic responses of living systems to pathophysiological stimuli via multivariate statistical analysis of biological NMR spectroscopic data, Xenobiotica 29 (1999) 1181–1189.
[13] P.Y. Yin, P. Mohemaiti, J. Chen, X.J. Zhao, X. Lu, A. Yimiti, H. Upur, G.W. Xu, Serum metabolic profiling of abnormal savda by liquid chromatography/mass spectrometry, J. Chromatogr. B 871 (2008) 322–327.
[14] M. Kellert, S. Wagner, U. Lutz, W.K. Lutz, Biomarkers of furan exposure by metabolic profiling of rat urine with liquid chromatography–tandem mass spectrometry and principal component analysis, Chem. Res. Toxicol. 21 (2008) 761–768.
[15] N.J. Li, W.T. Liu, W. Li, S.Q. Li, X.H. Chen, K.S. Bi, P. He, Plasma metabolic profiling of Alzheimer's disease by liquid chromatography/mass spectrometry, Clin. Biochem. 43 (2010) 992–997.
[16] T.G. Huo, S. Cai, X.M. Lu, Y. Sha, M.Y. Yu, F.M. Li, Metabonomic study of biochemical changes in the serum of type 2 diabetes mellitus patients after the treatment of metformin hydrochloride, J. Pharm. Biomed. Anal. 49 (2009) 976–982.
[17] Q. Zhang, X.K. Li, X. Cui, P.P. Zuo, D-galactose injured neurogenesis in the hippocampus of adult mice, Neurol. Res. 27 (2005) 552–556.
[18] X. Cui, P.P. Zuo, Q. Zhang, X.K. Li, Y.Z. Hu, J.G. Long, Chronic systemic D-galactose exposure induces memory loss, neurodegeneration, and oxidative damage in mice: protective effects of R-alpha-lipoic acid, J. Neurosci. Res. 84 (2006) 647–654.
[19] J.Y. Zheng, Y.R. Fu, M. Li, K.S. Gao, X.G. Zhang, Effect of LTA isolated from bifidobacteria on D-galactose-induced aging, Exp. Gerontol. 44 (2009) 760–765.
[20] S. Wiklund, E. Johansson, E.J. Mellerowicz, U. Edlund, J.P. Shockcor, J. Gottfries, T. Moritz, J. Trygg, Visualization of GC/TOF-MS-based metabolomics data for identification of biochemically interesting compounds using OPLS class models, Anal. Chem. 80 (2008) 115–122.
[21] E.S. Lee, C.G. Charlton, 1-Methyl-4-phenyl-pyridinium increases S-adenosyl-L-methionine dependent phospholipid methylation, Pharmacol. Biochem. Behav. 70 (2001) 105–114.
[22] M.E. Venable, J.Y. Lee, M.J. Smyth, A. Bielawska, L.M. Obeid, Role of ceramide in cellular senescence, J. Biol. Chem. 270 (1995) 30701–30708.
[23] Y.A. Hannun, L.M. Obeid, The ceramide-centric universe of lipid-mediated cell regulation: stress encounters of the lipid kind, J. Biol. Chem. 277 (2002) 25847–25850.
[24] H. Sawai, Y.A. Hannun, Ceramide and sphingomyelinases in the regulation of stress responses, Chem. Phys. Lipids 102 (1999) 141–147.
[25] G. van Meer, J.C. Holthuis, Sphingolipid transport in eukaryotic cells, Biochim. Biophys. Acta 1486 (2000) 145–170.
[26] C. Perrotta, P.C. De, S. Falcone, C. Sciorati, E. Clementi, Nitric oxide, ceramide and sphingomyelinase-coupled receptors: a tale of enzymes and messengers coordinating cell death, survival and differentiation, Life Sci. 77 (2005) 1732–1739.
[27] L.M. Obeid, Y.A. Hannun, Ceramide, stress, and a "LAG" in aging, Sci Aging Knowl. Environ. 2003 (2003) PE27.